



LAWRENCE  
LIVERMORE  
NATIONAL  
LABORATORY

UCRL-TR-205760

# Measurement of $^{150}\text{Sm}(n, 2\gamma_i)$ $^{149}\text{Sm}$ cross sections between threshold and 20 MeV

*J.R. Cooper, J.A. Becker, D. Dashdorj, F.S.  
Dietrich, P.E. Garrett, R. Hoffman, W. Younes*

**July 2004**

This document was prepared as an account of work sponsored by an agency of the United States Government. Neither the United States Government nor the University of California nor any of their employees, makes any warranty, express or implied, or assumes any legal liability or responsibility for the accuracy, completeness, or usefulness of any information, apparatus, product, or process disclosed, or represents that its use would not infringe privately owned rights. Reference herein to any specific commercial product, process, or service by trade name, trademark, manufacturer, or otherwise, does not necessarily constitute or imply its endorsement, recommendation, or favoring by the United States Government or the University of California. The views and opinions of authors expressed herein do not necessarily state or reflect those of the United States Government or the University of California, and shall not be used for advertising or product endorsement purposes.

# Measurement of $^{150}\text{Sm}(n,2n\gamma_i)^{149}\text{Sm}$ cross sections between threshold and 20 MeV

J. R. Cooper,\* J. A. Becker, D. Dashdorj, F. S. Dietrich,  
P. E. Garrett,\*\* R. Hoffman, W. Younes

*Lawrence Livermore National Laboratory, Livermore, CA 94551*

R. O. Nelson, M. Devlin, N. Fotiades

*Los Alamos National Laboratory, Los Alamos, NM 87545*

## Abstract

Absolute partial  $\gamma$ -ray cross sections for the production of discrete  $\gamma$ -rays from the reaction  $^{150}\text{Sm}(n,2n\gamma_i)^{149}\text{Sm}$  were measured using the GEANIE  $\gamma$ -ray spectrometer coupled with the intense white neutron source at WNR/LANSCE. The measurements were made for incident neutron energies between threshold (8.04 MeV) and 20 MeV. The partial cross sections for 21  $\gamma$ -rays were extracted from the data. Of these, 17 were compared to calculations performed using the enhanced Hauser-Feshbach code STAPRE. The partial  $\gamma$ -ray cross sections of the observed parallel decay paths to the ground state were summed, forming a lower bound for the (n,2n) reaction channel. A combination of theory and experiment was then used to deduce the (n,2n) reaction channel cross section.

## Introduction

Recent enhanced Hauser-Feshbach calculations of the (n,2n) reaction cross section in the mass 150 region show a systematic deviation [1] from experimental results. The calculated cross sections increase more rapidly with neutron energy than was observed experimentally. For example, Figure 1 shows the calculation of the  $^{150}\text{Sm}(n,2n)^{149}\text{Sm}$  reaction compared to experimental results reported in Reference [2], which were obtained using a method employing a large Gd loaded liquid scintillation detector [3].

This paper presents the results of a recent experiment to investigate the discrepancy by measuring the  $^{150}\text{Sm}(n,2n)^{149}\text{Sm}$  reaction cross section via a different technique [4-11]. First, partial  $\gamma$ -ray cross sections,  $^{150}\text{Sm}(n,2n\gamma_i)^{149}\text{Sm}$ , were measured using the GERmanium Array for Neutron-Induced Excitations (GEANIE) [12,13], located at the Weapons Neutron Research (WNR) facility [14] at the Los Alamos Neutron Science Center (LANSCE). Then the partial  $\gamma$ -ray cross sections of  $\gamma$ -rays that decay in parallel to the ground state (without double counting) were summed. This experimental sum was multiplied by the ratio of the calculated reaction channel cross section to the calculated summed parallel paths partial  $\gamma$ -ray cross section. This combination of theory and experiment gives the  $^{150}\text{Sm}(n,2n)^{149}\text{Sm}$  reaction channel cross section.

## Experimental Setup

The experiment was performed over a 10-day period during September and October of 2002 at the WNR/LANSCE facility at Los Alamos National Laboratory. Neutrons were produced by a spallation reaction on a natural tungsten target driven by a 3-4  $\mu\text{A}$  800 MeV proton beam. The pulsed proton beam was bunched into sub-nanosecond wide pulses each 1.8  $\mu\text{s}$  apart. This beam structure was delivered for 625  $\mu\text{s}$  producing a macropulse. Macropulses were delivered at a rate of 100 Hz giving a total duty cycle of 6%. The Sm target was located 20.34 m from the spallation target allowing time-of-flight measurement of the incident-neutron energy. The neutron beam was collimated to a beam diameter of 1.5 cm (full-width-half-maximum) at the target position. The neutron fluence was measured with a  $^{235}\text{U}$  and  $^{238}\text{U}$  fission chamber [15] located 18.48 m from the spallation target.

The 95.6(1)% enriched  $^{150}\text{Sm}_2\text{O}_3$  target was cylindrical in shape with a diameter of 2.54 cm, and contained 7500 mg of  $^{150}\text{Sm}$  about 0.3 cm thick. The target was placed at the focal point of the  $\gamma$ -ray array, GEANIE, with the plane of the target face perpendicular to the beam direction. At the time of the experiment, GEANIE consisted of 11 Compton-suppressed planar germanium detectors and 14 coaxial Ge detectors (9 Compton-suppressed and 5 unsuppressed). The 5 coaxial detectors without anti-Compton shields were not used in the data analysis.

For approximately 1 day of the 10-day experiment, four 0.05-mm thick  $^{\text{nat}}\text{Fe}$  foils were placed on each side of the target. The  $^{\text{nat}}\text{Fe}(n,n'\gamma_i=846.8 \text{ keV})^{\text{nat}}\text{Fe}$  cross section is 705 mb [16] at  $E_n = 14.5 \text{ MeV}$  as measured relative to  $^{\text{nat}}\text{Cr}(n,n'\gamma_i=1434 \text{ keV})$ . The cross section for the  $^{\text{nat}}\text{Cr}$  1434-keV gamma-ray from the evaluation of Simakov *et al.* is 695 (35) mb. (Note that Simakov *et al.* evaluate the  $^{\text{nat}}\text{Fe}$  846.8-keV  $\gamma$ -ray cross section to be 785 (48) mb [17].)

Data were recorded for  $\gamma$ -ray energies between 40 keV and 1 MeV in the planar detectors and 40 keV and 2.6 MeV in the coaxial detectors. Timing information was recorded relative to the beam micropulse and scalar data were taken to allow determination of the detector dead time. A total of  $1.47 \times 10^8$  and  $8.9 \times 10^7$  events were recorded in the coaxial and planar detectors respectively.

## Data Analysis

The partial  $\gamma$ -ray cross section of a particular  $\gamma_i$  was calculated using the following formula:

$$\sigma_{\text{partial}\gamma\text{-ray}} = \frac{N_{\gamma} C_{\gamma} (1 + \alpha_{\text{tot}})}{\epsilon_{\gamma} (LT)_{\gamma}} \times \frac{\epsilon_{FC} (LT)_{FC}}{N_{FC}} \times \frac{1}{t}, \quad [1]$$

where  $N_{\gamma}$  is the number of counts in the photopeak of  $\gamma_i$  in the  $\gamma$ -ray detector array,  $C_{\gamma}$  is a correction factor for angular distribution effects of  $\gamma_i$ ,  $\alpha_{\text{total}}$  is the total internal conversion coefficient of  $\gamma_i$ ,  $\epsilon_{\gamma}$  is the  $\gamma$ -ray detector array efficiency at the  $\gamma$ -ray energy  $E_{\gamma_i}$ ,  $(LT)_{\gamma}$  is the live time of the  $\gamma$ -ray detector array,  $\epsilon_{\text{FC}}$  is the efficiency of the fission chamber,  $(LT)_{\text{FC}}$  is the live time of the fission chamber,  $N_{\text{FC}}$  is the number of counts in the fission chamber, and  $t$  is the target thickness in atoms/mb. Data from the coaxial and planar germanium detectors were analyzed independently and the partial  $\gamma$ -ray cross sections were compared to ensure that consistent results were obtained.

The number of counts in the photopeak,  $N_{\gamma}$ , was determined using the software package XGAM developed at Lawrence Livermore National Laboratory by Younes. A fitting routine was used to fit the peak areas, peak shapes, and background for the entire  $\gamma$ -ray spectrum collected in the time-of-flight range corresponding to neutron energies between 1 and 20 MeV. Then, with the peak positions and peak shapes fixed, spectra for time-of-flight bins (corresponding to a particular neutron energy range) were fitted allowing only the area of the peak to vary. The peak areas,  $N_{\gamma}$ , determined in this way for each time-of-flight bin were used in the calculation of the partial  $\gamma$ -ray cross section. More information on the software and data analysis techniques can be found in Reference [18].

The fission chamber and  $\gamma$ -ray detector live times were calculated by dividing the number of events converted by the ADC by the number of events in the associated scalar. The live times in this experiment for the  $^{238}\text{U}$  fission chamber, coaxial detectors and planar detectors were 16.3%, 12.2%, and 13.8% respectively. This was much smaller than typical 60% live times due to a faulty latch in the data acquisition system.

The  $\gamma$ -ray efficiencies were calculated through Monte-Carlo simulations [19,20] that were normalized and validated with point-source and extended-source measurements. It should be noted that the Monte-Carlo calculation for the coaxial detectors is performed only for  $\gamma$ -ray energies above 300 keV and measurements were used to generate the coaxial detector efficiency below this energy. This was necessary to account for the use of slow-rise-time rejection in the constant-fraction discriminators. However, as will be shown below, excellent agreement is obtained with the planar detectors, for which the array efficiency is calculated down to 60 keV.

The internal conversion coefficients were obtained from the NUDAT [21] compilation. The target thickness was 0.00568 atoms/barn and a 5% uncertainty was assigned due to the uncertainty in the uniformity of the powdered sample in the container. The number of counts in the  $^{238}\text{U}$  fission chamber,  $N_{\text{FC}}$ , was obtained from the time of flight projection spectrum with a threshold set above the alpha decay energy. Angular distribution corrections were not made in this analysis. During this experiment the detectors were arranged to obtain wider angular coverage with the planar detectors to improve the angular distribution

data. However, differences of the angular distributions from isotropy were hard to observe, and so no attempt was made to correct the data.

## Iron Line Analysis

For approximately one day, four 0.05-mm thick  $^{nat}\text{Fe}$  sheets were placed on both sides of the Sm target. The data with the Fe sheets in place were analyzed and the partial  $\gamma$ -ray cross section for the  $^{56}\text{Fe}$ , 846 keV,  $2_1^+ \rightarrow 0_1^+$  transition was extracted. The results of the analysis are shown in Figure 2 along with the  $^{56}\text{Fe}$  results from a previous GEANIE experiment (to measure partial  $\gamma$ -ray cross sections of neutron induced reactions on  $^{75}\text{As}$ ) [22]. The partial  $\gamma$ -ray cross section, as determined from the planar detectors, was approximately 5% larger than the results from the previous experiment. Therefore, the partial cross section measurement using the planar detectors was consistent, within errors, with previous work.

The situation with the coaxial detectors was not as good. The resulting  $^{56}\text{Fe}$  partial  $\gamma$ -ray cross section was significantly larger than the result from the planar detectors and from the previous experiment. The discrepancy may be caused by systematic errors in  $N_\gamma$ ,  $C_\gamma$ ,  $LT_\gamma$ , or  $\epsilon_\gamma$ . A systematic error in  $N_\gamma$  due to the neutron-induced peak at 834 keV was investigated and found not to account for the discrepancy. As discussed above,  $C_\gamma$  was not measured, but such a large difference in the angular distribution factor between the planar and coaxial detectors is unlikely. In addition, the angular distribution correction factor would show a dependence on incident neutron energy due to the neutron energy dependence of the nuclear alignment. As shown in the bottom panel of Figure 2, a neutron energy independent scale factor of 1.20(2) brings the results from the planar and coaxial detectors into agreement. The difference is likely due to changes in the detector positions that were not fully accounted for in correcting the gamma-ray attenuation in the sample.

It was decided to apply a correction factor of 1.20(2) to renormalize the coaxial  $^{56}\text{Fe}$  partial  $\gamma$ -ray cross section. The correction factor was determined using the maximum likelihood method and assuming neutron energy independence (data between 2 and 20 MeV was used in the fit). In addition,  $\gamma$ -ray energy independence of the correction factor was found when analyzing the partial  $\gamma$ -ray cross sections from the  $^{150}\text{Sm}(n,2n\gamma_i)^{149}\text{Sm}$  reaction, as will be shown below. All  $^{150}\text{Sm}(n,2n\gamma_i)^{149}\text{Sm}$  partial  $\gamma$ -ray cross sections from the coaxial detectors presented in this paper have been divided by a correction factor of  $1.20 \pm 0.02$ . Good agreement was obtained between the coaxial and planar detectors with the inclusion of a coaxial-correction factor.

## STAPRE Calculations

The enhanced Hauser-Feshbach code, STAPRE, was used to calculate  $^{150}\text{Sm}(n,2n\gamma_i)^{149}\text{Sm}$  partial  $\gamma$ -ray cross sections. The calculation includes pre-

equilibrium processes for the first emitted particle. The discrete level scheme for reaction channels of interest were used as input to STAPRE and levels up to 953 keV in  $^{149}\text{Sm}$  were included in the calculation. Details of the modeling procedure are given in Hoffman, et al. [24].

## Results

Twenty-one partial  $\gamma$ -ray cross sections from the  $^{150}\text{Sm}(n,2n)^{149}\text{Sm}$  reaction channel were measured with 17 from levels included in the STAPRE calculations. The results are shown in Figures 3, 4 and 5. A few of the lines are discussed in detail below.

- 1) The 350 keV  $\gamma$ -ray contains two components, one from the 636.5 keV level, and one from the 350.0 keV level. The sum of the calculated partial cross section is shown in Figure 3.
- ~~1~~2) The 281.3 keV  $\gamma$ -ray was extremely weak and in a region of the spectrum with a background that was difficult to fit. The results are included in Figure 3; however, a systematic error on the order of 5 mb is evident between the planar and coaxial detectors.
- ~~1~~3) The experimentally measured branching ratio from the 664.1-keV level as determined by the partial  $\gamma$ -ray cross section of the 378.3 and 664.1 keV line is in agreement with the value in NUDAT.
- ~~1~~4) The experimentally measured branching ratio from the 789.5- keV level as determined by the partial  $\gamma$ -ray cross section of the 125.4- and 198.6-keV line is not in agreement with the value in NUDAT. The cause for the disagreement is not known.

As shown in Figures 3 and 4, STAPRE over predicts the partial  $\gamma$ -ray cross sections of some levels, while under predicting others. Often incorrect predictions of individual partial  $\gamma$ -ray cross sections can be reconciled to the data by summing parallel paths to the ground state, in effect, averaging. In  $^{149}\text{Sm}$ , the first excited state is at 22.5 keV and decays through internal conversion; therefore, the sum of parallel paths to the ground state and first-excited state is needed.

Table 1 gives a list of the levels from which  $\gamma$ -ray decays to the ground state or first excited state were observed. Both gamma rays were observed from the 277.1, 350.0 keV levels. Only one of the  $\gamma$ -rays was observed from the other levels due to contamination from a nearby peak or lack of intensity. To account for the missing intensity, the experimental and calculated partial  $\gamma$ -ray cross sections were multiplied by a correction factor determined from the branching ratios. The multiplication factor is given by the sum of the branching ratio to the ground and first excited states divided by the branching ratio of the observed transition. Using this multiplication factor, Figure 6 shows the summed partial  $\gamma$ -ray cross sections from the levels given in Table 1. This also gives a lower bound of the

$^{150}\text{Sm}(n,2n\gamma_i)^{149}\text{Sm}$  reaction cross section. It should be noted that a constant factor of 40 mb was subtracted from the experimental data in order to bring the cross section to zero below threshold. This subtraction is needed due to an inexact fit to the background.

The reaction channel cross section can be calculated from the experimental summed parallel paths partial  $\gamma$ -ray cross sections. This is done by multiplying the experimental data (the weighted average of the planar and coaxial detectors was used) by a ratio of calculated cross sections. The ratio is the reaction channel cross section divided by the calculated summed parallel paths partial  $\gamma$ -ray cross section. The result is listed in Appendix 1 and shown in Figure 7 along with the calculated  $^{150}\text{Sm}(n,2n)^{149}\text{Sm}$  reaction cross section and the data from Reference [2].

In general, the results are in good agreement with the previous experimental results. There is some disagreement at neutron energies between 14-15 MeV, but overall, the results from this experiment support the previous experimental results[2].

## ACKNOWLEDGMENTS

Hospitality of the LANL Host Group LANSCE-3 is appreciated by the LLNL visiting staff. This work was performed under the auspices of the U.S. Department of Energy by the University of California, Los Alamos National Laboratory under contract no. W7405-ENG-36 and Lawrence Livermore National Laboratory under contract no. W7405-ENG-48, and benefited from the use of the Los Alamos Neutron Science Center supported under contract no. W-7405-ENG-36.



## References

- \* Present address: USEC Inc., PO Box 628 MS-2227, Piketon, OH 45661.
- \*\* Present address: Physics Department, University of Guelph, Guelph, Ontario, Canada, N1G 2W1.
- [1] R.D. Hoffman, Lawrence Livermore National Laboratory, private communication.
- [2] J. Frehaut, A. Bertin, R. Bois, J. Jary, *Symposium on Neutron Cross Sections from 10-50 MeV*, Upton, NY (USA), May 12-14, 1980.
- [3] J. Frehaut, *Nuclear Instruments and Methods* 135, 511 (1976).
- [4] N. Fotiades, G. D. Johns, R. O. Nelson, M. B. Chadwick, M. Devlin, M. S. Wilburn, P. G. Young, J. A. Becker, D. E. Archer, L. A. Bernstein, P. E. Garrett, C. A. McGrath, D. P. McNabb, and W. Younes, *Measurements and calculations of  $^{238}\text{U}(n, xn\gamma)$  partial  $\gamma$ -ray cross sections*, Phys. Rev. C 69, 024601 (2004).
- [5] P. E. Garrett, D. E. Archer, J. A. Becker, L. A. Bernstein, K. Hauschild, E. A. Henry, D. P. McNabb, M. A. Stoyer, W. Younes, G. D. Johns, R. O. Nelson, W. S. Wilburn, *Rotational Bands and isomeric states in  $^{175}\text{Lu}$* , Phys. Rev. C 69, 017302 (2004).
- [6] P. E. Garrett, W.E. Ormand, W. Younes, J.A. Becker, L.A. Bernstein, R.O. Nelson, M. Devlin, N. Fotiades, *Revised Cross Sections for  $n + ^{89}\text{Y}$  for  $E_n < 20$  MeV*, UCRL-MI-200319, 2003.
- [7] P. E. Garrett, W. Younes, J. A. Becker, L. A. Bernstein, E. M. Baum, D. P. DiPrete, R. A. Gatenby, E. L. Johnson, C. A. McGrath, S. W. Yates, M. Devlin, N. Fotiades, R. O. Nelson, and B. A. Brown, *Nuclear structure of the closed subshell nucleus  $^{90}\text{Zr}$  studied with the  $(n, n'\gamma)$  reaction*, Phys. Rev. C 68 024312 (2003).
- [8] L. A. Bernstein, J. A. Becker, P. E. Garrett, W. Younes, D. P. McNabb, D. E. Archer, C.A. McGrath, H. Chen, W. E. Ormand, M.A. Stoyer, R. O. Nelson, M.B. Chadwick, G.D. Johns, W. S. Wilburn, M. Devlin, D. M. Drake and P.G. Young, *The  $^{239}\text{Pu}(n, 2n)$  cross section deduced using a combination of experiment and theory*, Phys. Rev. C 65, 021601(R) (2002).
- [9] E. Tavukcu, L. A. Bernstein, K. Hauschild, J. A. Becker, P. E. Garrett, C.A. McGrath, D. P. McNabb, W. Younes, M.B. Chadwick, R. O. Nelson, G.D. Johns, and G.E. Mitchell,  *$^{196}\text{Pt}(n, xnyp\gamma)$  reactions using spallation neutrons from  $E_n = 1$  to 250 MeV*, Phys. Rev. C 64, 054614 (2001).

- [10] P. E. Garrett, L. A. Bernstein, J. A. Becker, K. Hauschild, C.A. McGrath, D. P. McNabb, W. Younes, M.B. Chadwick, G.D. Johns, R. O. Nelson, W. S. Wilburn, E. Tavukcu, S.W. Yates,  *$^{92}\text{Mo}(n,xnypz\gamma)$  reactions for neutron energies up to 250 MeV*, Phys. Rev. C 62, 054608-1 (2000).
- [11] P. E. Garrett, L. A. Bernstein, J. A. Becker, K. Hauschild, C.A. McGrath, D. P. McNabb, W. Younes, E. Tavukcu, G.D. Johns, R. O. Nelson, W. S. Wilburn and S.W. Yates, *States in  $^{92}\text{Mo}$  observed with the  $(n,n'\gamma)$  reaction with spallation neutrons*, Phys. Rev. C 62, 014307 (2000).
- [12] J.A. Becker and R.O. Nelson, *New Physics Opportunities with GEANIE at LANSCE/WNR*, Nuclear Physics News, 7 (1997) 11. LA-UR-97-1080.
- [13] R.O. Nelson, J.A. Becker, D.E. Archer, L.A. Bernstein, G.D. Johns, W.S. Wilburn, W. Younes, D.M. Drake, R.S. Rundberg, S.A. Wender, K. Hauschild, S.W. Yates and P.E. Garrett, *GEANIE at WNR/LANSCE -- a New Instrument for Neutron Science*, Italian Physical Society Conference Proceedings 59, p. 445, 1997, International Conference on Nuclear Data for Science and Technology, May 19-24, 1997, Trieste, Italy.
- [14] P. W. Lisowski, C. D. Bowman, G. J. Russell, and S. A. Wender, *The Los Alamos National Laboratory Spallation-Neutron Sources*, Nucl. Sci. Eng. 106, 208 (1990).
- [15] S.A. Wender, S. Balestrini, A. Brown, R.C. Haight, C.M. Laymon, T.M. Lee, P.W. Lisowski, W. McCorkle, R.O. Nelson, W. Parker, and N. Hill, Nucl. Inst. Meth. Phys. Res. A 336, 226 (1993).
- [16] Ron Nelson, Los Alamos National Laboratory, LAUR, in progress.
- [17] S.P. Simakov, A. Pavlik, H. Vonach, S. Hlavac, *Status of Experimental and Evaluated Discrete Gamma-Ray Production at  $E_n=14.5$  MeV*, Tech. Rep. INDC(CCP)-413, International Atomic Energy Agency (1998).
- [18] W. Younes, J.A. Becker, L.A. Bernstein, P.E. Garrett, C.A. McGrath, D.P. McNabb, R.O. Nelson, M. Devlin, N. Fotiades, G.D. Johns, *The  $^{235}\text{U}(n,2n\gamma)$  Yrast Partial Gamma-Ray Cross Sections: A Report on the 1998 and 1999 GEANIE Data Analysis Techniques*, Tech. Rep. UCRL-ID-140313, LLNL (2000).
- [19] D.P. McNabb, *Uncertainty Budget and Efficiency Analysis for the  $^{239}\text{Pu}(n,2n\gamma)$  Partial Reaction Cross Section Measurements*, Tech. Rep. UCRL-ID-139906, LLNL (1999).
- [20] J.F. Briesmeister, *A General Monte-Carlo Code for Neutron and Photon Transport*, Tech. Rep. LA-7396-M-Rev. 2, LANL (1986).

- [21] <http://www.nndc.bnl.gov/nndc/nudat/>
- [22] W. Younes, P.E. Garrett, J.A. Becker, L.A. Bernstein, W.E. Ormand, F.S. Dietrich, R.O. Nelson, M. Devlin, N. Fotiades, *Analysis of  $^{75}\text{As}(n,xn\gamma)$  cross sections*, Tech. Rep. LLNL (2003) manuscript in preparation.
- [23] R. Hoffman, et al., UCRL-TR-205563(2004).

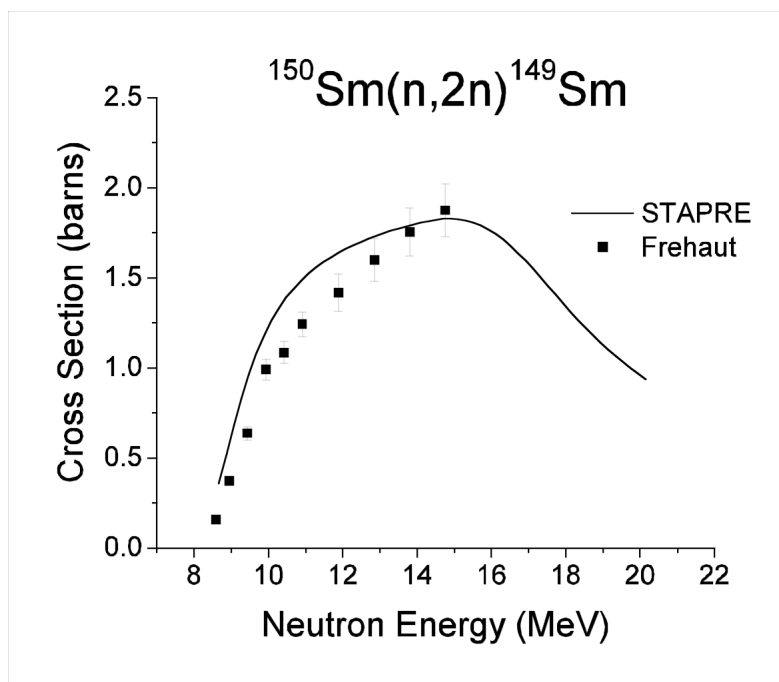


**Figure 1.** STAPRE (n,2n) calculations (solid line) show a systematic deviation from the experimental data (squares) as illustrated by the  $^{150}\text{Sm}(n,2n)^{149}\text{Sm}$  reaction.

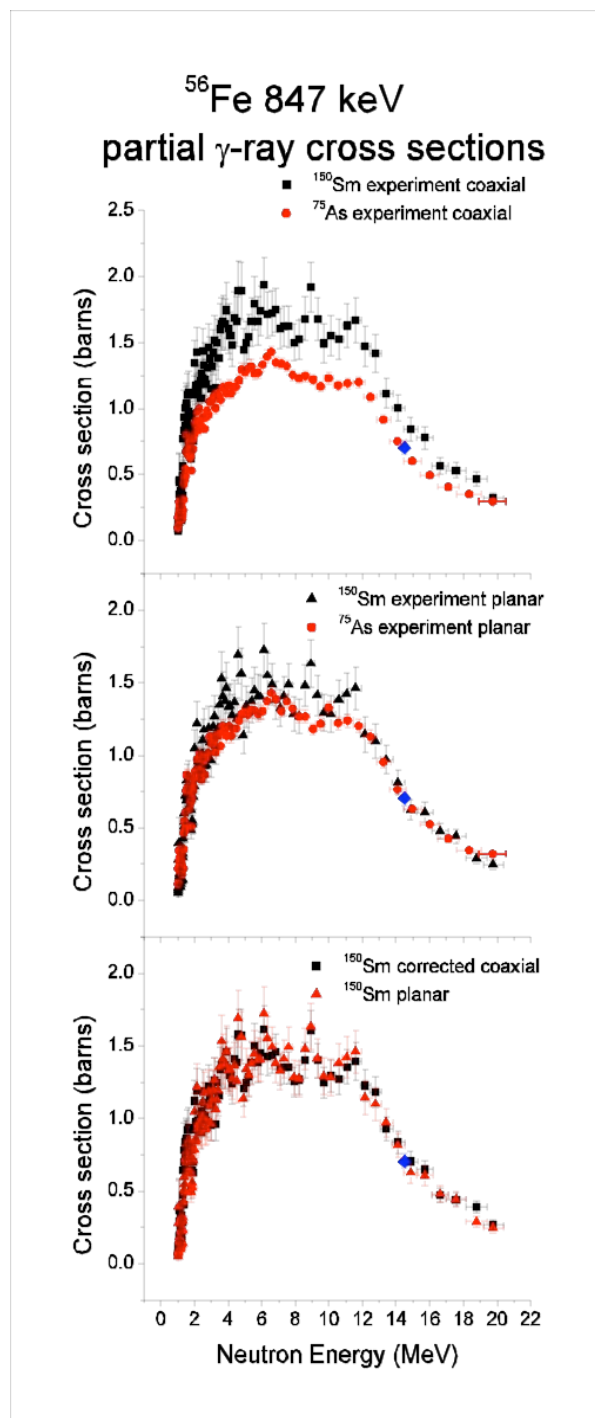


**Figure 2.** The top panel shows the  $^{56}\text{Fe}$ , 846 keV, partial  $\gamma$ -ray cross section as measured by the coaxial detectors during the experiment to measure neutron induced reactions on  $^{150}\text{Sm}$  (squares) and  $^{75}\text{As}$  (circles) while the middle panel shows the results from the planar detectors ( $^{150}\text{Sm}$  triangles and  $^{75}\text{As}$  circles). The bottom panel compares the results from the coaxial detectors, divided by a factor of 1.20, to the results from the planar detectors. The diamond at 14.5 MeV shows the 705 mb data point reported in Reference [16].

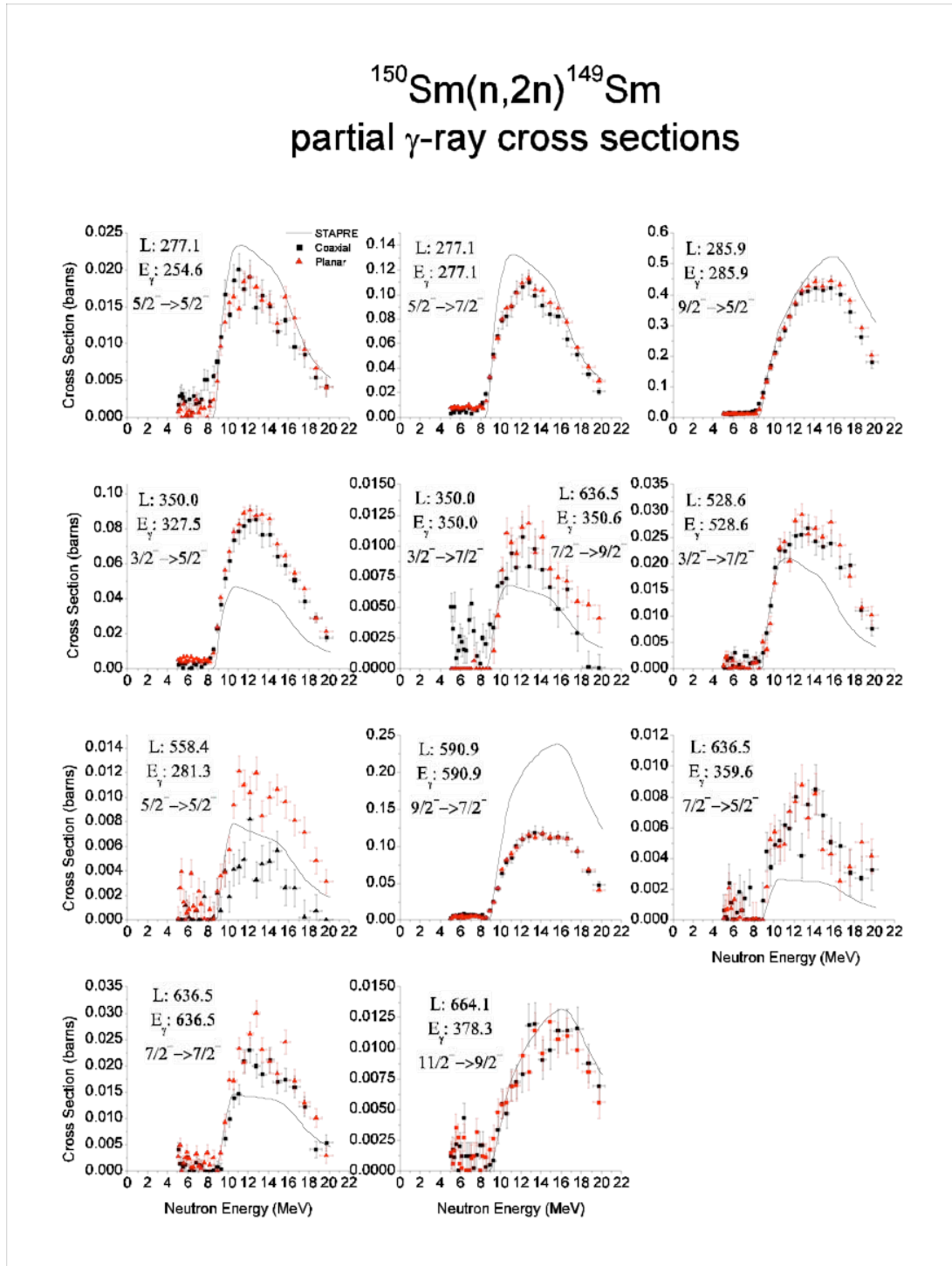


**Figure 3.** Partial  $\gamma$ -ray cross sections from the reaction  $^{150}\text{Sm}(n,2n)^{149}\text{Sm}$  as measured using the coaxial detectors (squares) and planar detectors (triangles). STAPRE calculations are shown by the solid line. The energy level,  $L$ ,  $\gamma$ -ray energy,  $E_\gamma$ , and spin and parity of the initial and final levels are indicated.

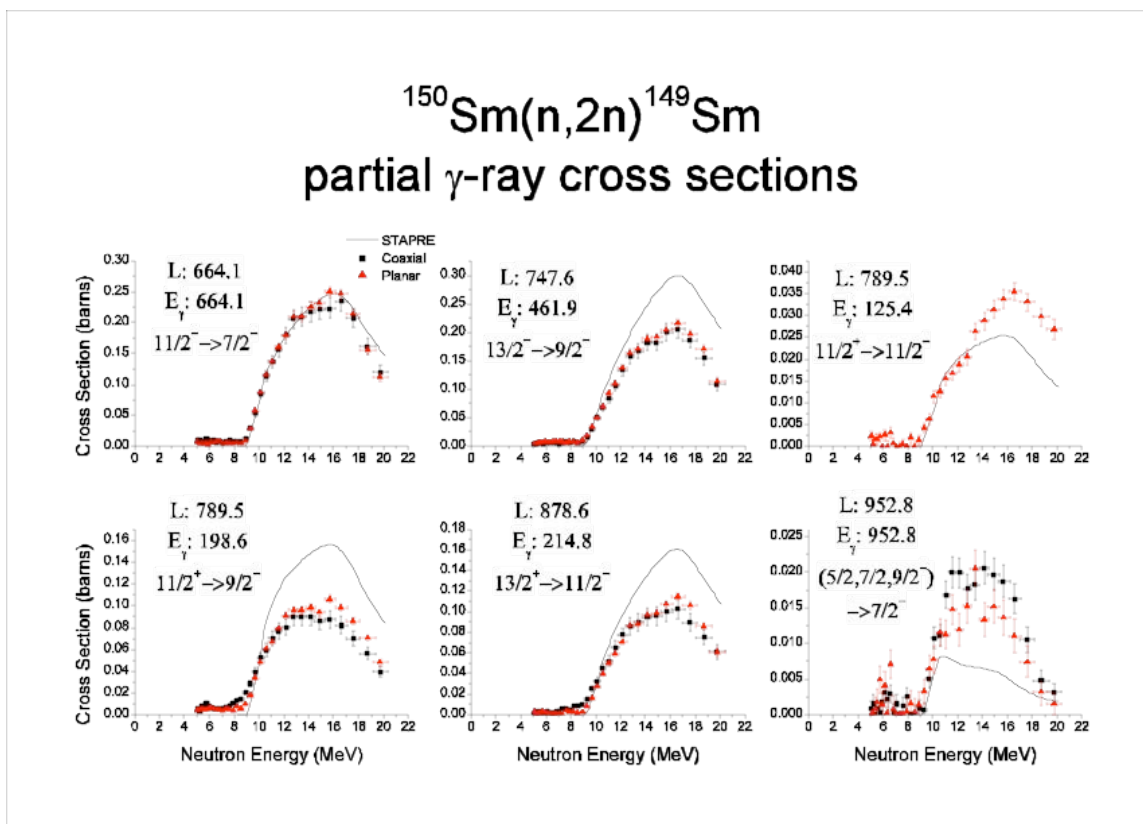


**Figure 4.** More partial  $\gamma$ -ray cross sections from the reaction  $^{150}\text{Sm}(n,2n\gamma)^{149}\text{Sm}$  as measured using the coaxial detectors (squares) and planar detectors (triangles). STAPRE calculations are shown by the solid line.

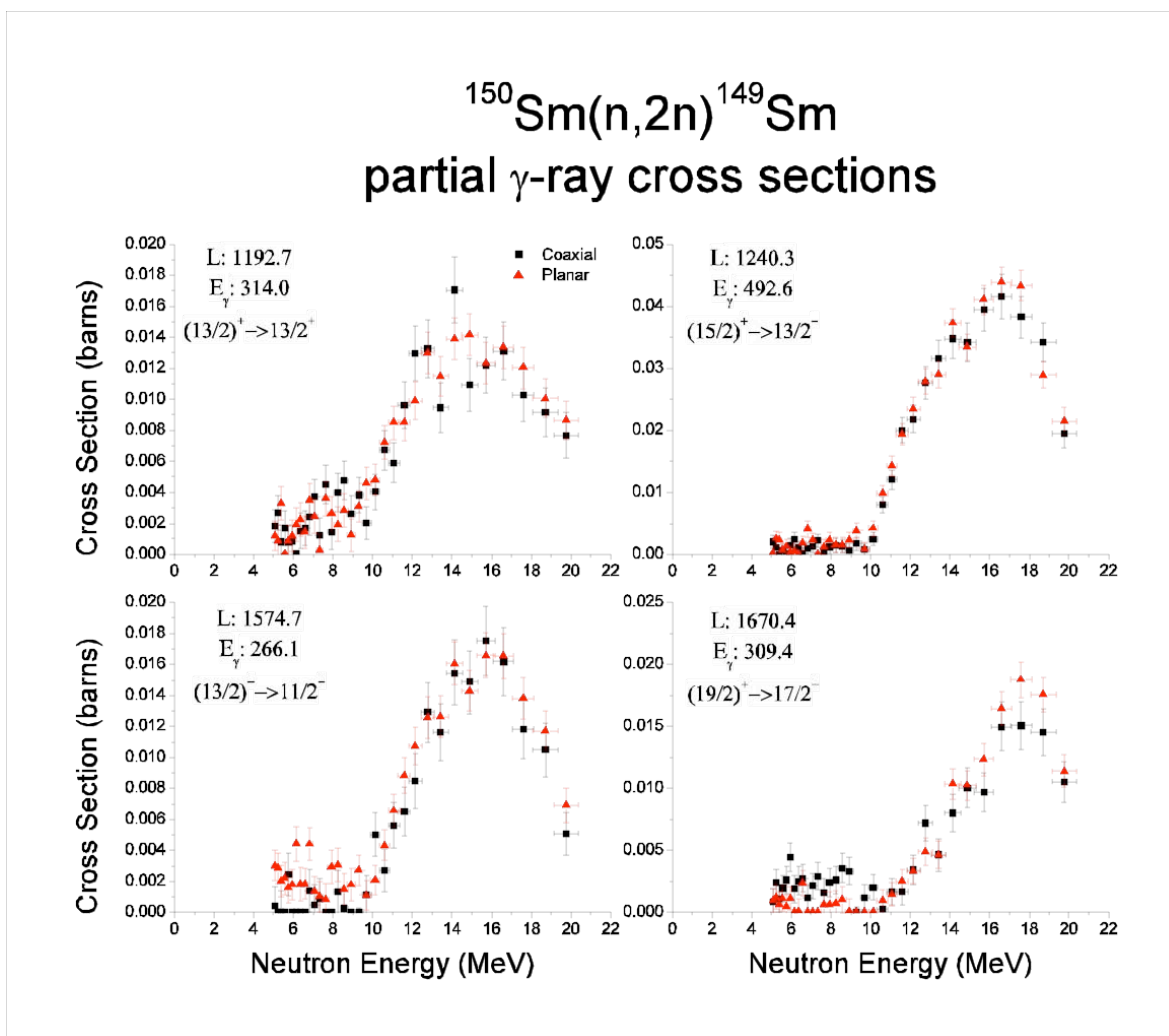


**Figure 5.** Partial  $\gamma$ -ray cross sections from the reaction  $^{150}\text{Sm}(n,2n\gamma)^{149}\text{Sm}$  as measured using the coaxial detectors (squares) and planar detectors (triangles). These levels were not included in the STAPRE calculations. The energy level, L,  $\gamma$ -ray energy,  $E_\gamma$ , and spin and parity of the initial and final levels are indicated.



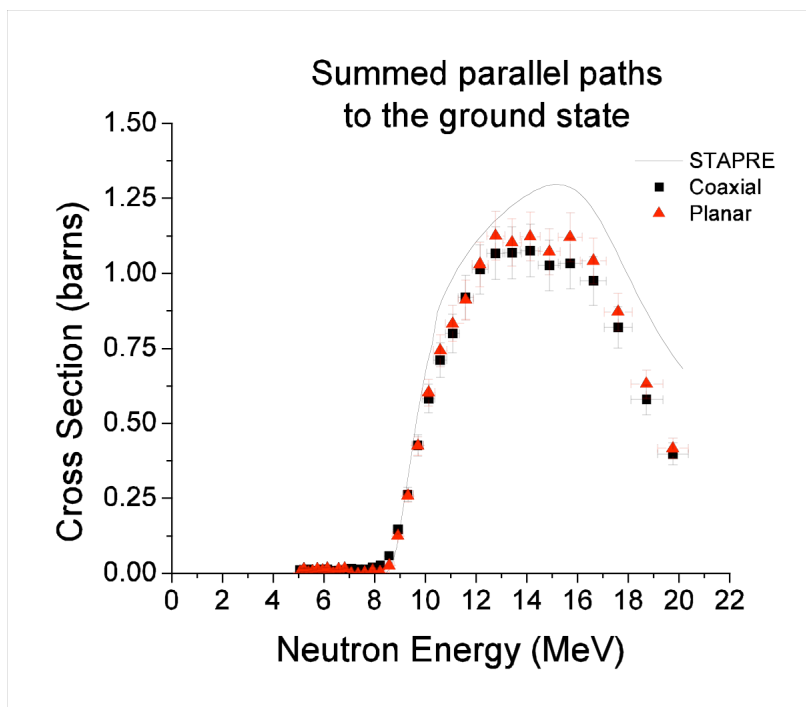


**Figure 6.** The summed parallel paths to the ground state; coaxial detectors (squares) planar detectors (triangles), and STAPRE calculations (solid line).

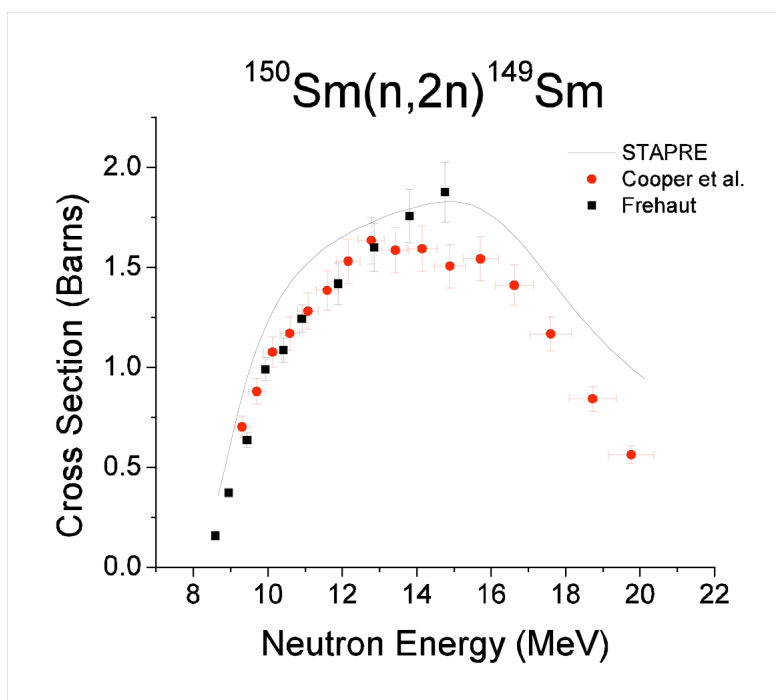


**Figure 7.** The  $^{150}\text{Sm}(n,2n)^{149}\text{Sm}$  reaction cross section from this experiment (circles) Frehaut (squares) and STAPRE calculations (solid line).

**Table 1.** Gamma rays included in the parallel paths to the ground state and multiplication factors needed to account for unobserved transitions.

Level Energy (keV)	$\gamma$ -ray Energy (keV)	Observed	Multiplication Factor
277.1	277.1	Yes	1.00
	254.6	Yes	1.00
285.9	285.9	Yes	1.00
	263.2	No	
350	350	Yes	1.00
	327.5	Yes	1.00
528.6	528.6	Yes	2.10
	506.1	No	
590.9	590.9	Yes	1.25
	568.4	No	
636.5	636.5	Yes	2.67
	613.9	No	
664.1	664.1	Yes	1.00
	NA		
952.8	952.8	Yes	1.68
	930.2	No	

## Appendix 1.

Table 2.  $^{150}\text{Sm}(n,2n)$  cross section deduced in this experiment, see Figure 7. The width of the neutron energy bin is given as  $\Delta E_n$ .

$E_n$ (MeV)	$\Delta E_n$ (MeV)	$\sigma(b)$	$\Delta\sigma(b)$
9.31	0.21	0.70	0.05
9.70	0.23	0.88	0.06
10.13	0.24	1.08	0.08
10.59	0.26	1.17	0.08
11.07	0.28	1.28	0.09
11.59	0.30	1.38	0.10
12.16	0.32	1.53	0.11
12.77	0.35	1.63	0.12
13.42	0.37	1.59	0.11
14.14	0.41	1.59	0.11
14.89	0.42	1.50	0.11
15.71	0.48	1.54	0.11
16.62	0.52	1.41	0.10
17.60	0.56	1.17	0.08
18.72	0.63	0.84	0.06
19.76	0.61	0.56	0.04